Transmission through Multiple Nanoscale Rings with Zeeman-split Quantum Dots

James B. Cutright, Yong S. Joe, and Eric R. Hedin
Center for Computational Nanoscience, Department of Physics and Astronomy
Ball State University
Muncie, IN
erhedin@bsu.edu

***Abstract*— A nanoscale ring structure, typically referred to as an Aharonov-Bohm (AB) ring, with a quantum dot (QD) embedded in each arm serves a unit cell in a chain-like structure. The transmission through the device is presented as a function of the number of rings in the chain. Zeeman-splitting of the QD energy levels is also modeled and its effects are analyzed. Distinct transmission bands form as the ring number increases. Zeeman splitting causes the number of bands to double, and to cross and diverge as the magnitude of the Zeeman effect increases. I-V plots show a transition from semi-conductor characteristics to ohmic properties as the Zeeman splitting approaches the nominal energy value of the QD's.**

Keywords-Aharonov-Bohm rings; quantum dots; Zeeman spin splitting; transmission; current-voltage

I. INTRODUCTION

Electron transmission through nanoscale ring structures with quantum dots (QD's) embedded in each arm have been the focus of theoretical and experimental research [1]. The phase coherence of the electrons is maintained during their passage through the ring and QD's, leading to possibility of studying interference and resonance effects, including Breit-Wigner and Fano type resonances.

The application of external magnetic fields to the structure can produce a combination of Aharonov-Bohm (AB) and Zeeman effects, which also introduce novel transmission resonances which facilitate spin-filtering [2]. Further, our recently investigated results on sharpened AB oscillations [3], and reversal of spin polarization due a small Zeeman splitting [4] for parallel double QD's in resonance suggest the applicability of such structures in the growing field of spintronics [5].

In this article, we study spin-polarized transmission through a series of asymmetric AB-ring interferometers; each with QD's embedded in the arms. We do this by incorporating the electron spin into a tight-binding Hamiltonian. We also assume that the spin degeneracy of the electrons is lifted by the Zeeman effects via application of an external, in-plane magnetic field (which precludes an AB phase shift).

II. MODEL AND METHOD OF ANALYSIS

A schematic of the model used in this work is shown in Fig. 1, which illustrates the spin-split QD's in each arm of a double ring. The rings are coupled to semi-infinite leads which are assumed to be spin-neutral, which can be accomplished, for example, by using materials for which the g-factor of the leads is much lower than for the QD's [6,7].

The tight-binding approximation to the Schrödinger equation, shown in (1), is used to computationally evaluate the transmission through the multiple-ring structure.

$$-\sum_{m} V_{n,m}\Psi_m + \varepsilon_n\Psi_n = E\Psi_n \qquad (1)$$

The inter-QD coupling integrals are set to V_n=0.1, and the couplings between sites in the 1-d leads are all set to V_o=1.0, which we use throughout the discussion as a unit of energy.

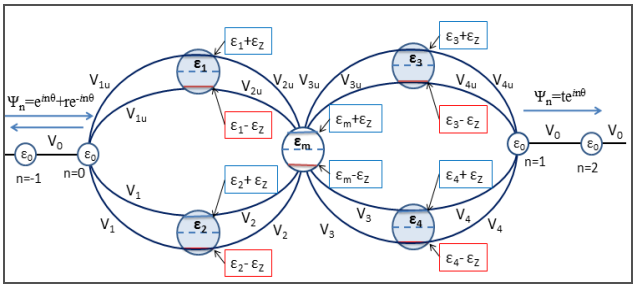

Figure 1. Sample schematic of a two ring system. Each ring consists of an A-B Ring with embedded quantum dots in each arm. Identical leads act as a source and drain for the system. A magnetic field, parallel to the plane of the rings, Zeeman splits the quantum dot energy levels. The incident and reflected wavefunctions are shown on the left, the transmitted on the right. Additional rings may be added in series.

The electron energy window is $-2V_o \le E \le 2V_o$, as set by the tight-binding dispersion relation for the uniform leads: $E = -2V_0\cos(\theta) + \varepsilon_0$, where $\theta = ka$, with a the inter-site spacing in the leads, and k the wavenumber. All upper QD site energies are set to $\varepsilon_n = 0.1$, all lower sites to $\varepsilon_n = -0.1$, and all other sites to $\varepsilon_n = \varepsilon_0 = 0.0$.

III. COMPUTATIONAL RESULTS

Typically, in a one ring system, two resonant peaks will appear, each located approximately at a value corresponding to the energy of one of the QD's. Additional pairs of peaks appear for each supplemental ring added (Fig. 2).

The new peaks are also symmetrically placed around zero energy, with their positions filling in a conduction band extending away from the QD site energy value. The conduction band formed by these resonant peaks is bound approximately by the energy window, $-0.3V_0 \le E \le 0.3V_0$, when there is no Zeeman splitting, with the band becoming more of a continuum as additional rings are added and individual resonant peaks narrow.

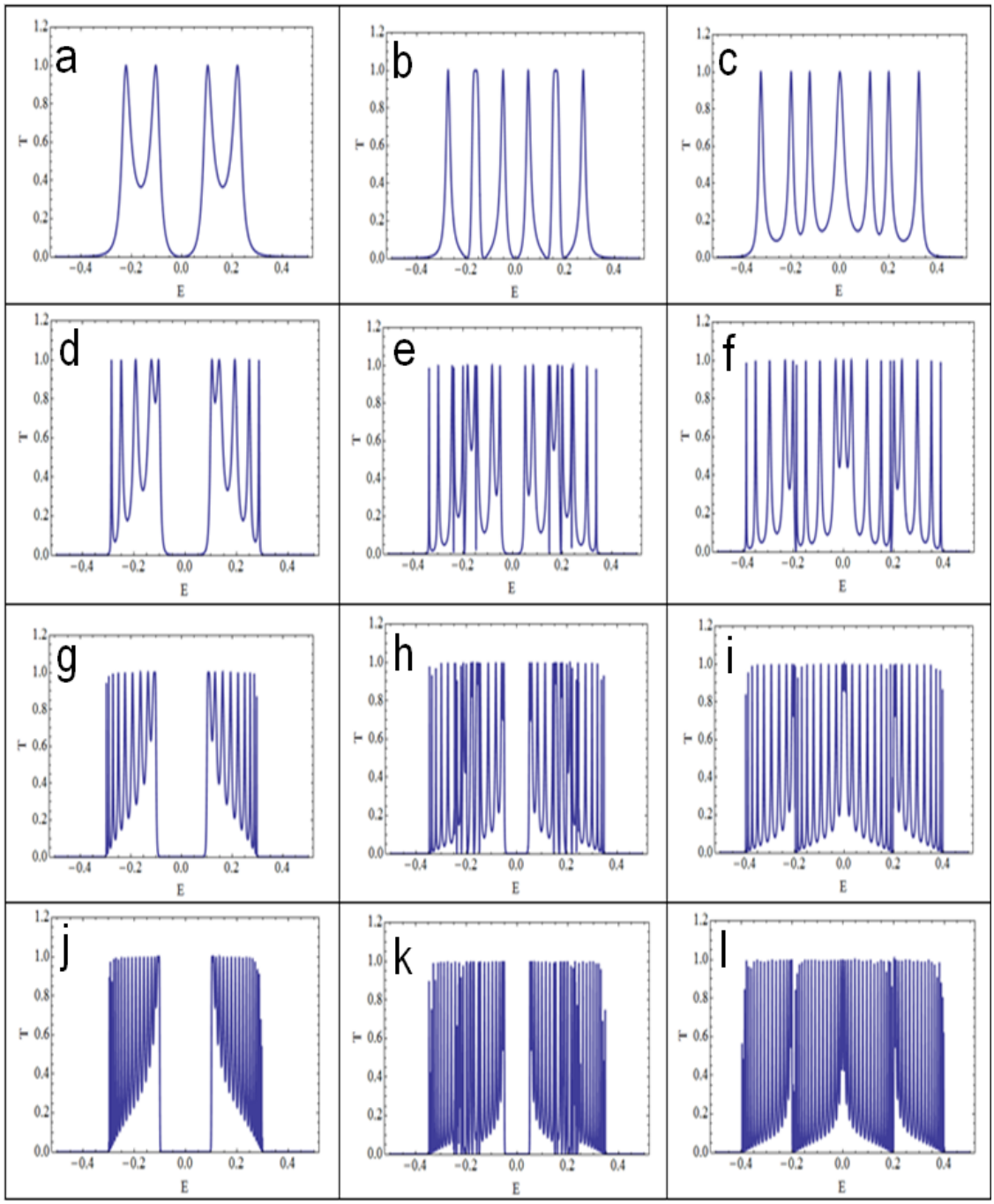

Figure 2. Transmission through multi-ring systems for two (a-c), five (d-f), ten (g-i), and twenty (j-l) ring structures. The leftmost graphs show no Zeeman splitting in the field. The central graphs are for a Zeeman split energy of 0.05, and the right most 0.1.

In each system, the number of rings determines how well defined the band gap is, with more rings providing higher definition of the band edges (Fig. 2, top to bottom). Measuring the location of the band gap edges for systems with high ring number reveals that the inner edges sit at energy values very close to that of the quantum dots (Fig. 2j). Applying the external field splits all the peaks, making the conduction band even more defined, but shrinking the band gap, until the band gap disappears when the energy of Zeeman splitting energy (ZSE) is on the order of the QD energy levels (see 2nd and 3rd columns of Fig. 2).

From the contour plot (Fig. 3a) it is evident that as the ZSE increases past that of the QD's, the system remains a conductor as the resonant peaks cross through each other. When the ZSE is about three times that of the QD energy, the system begins to transition to a semiconductor again, except with multiple band gaps (see the plots in Fig. 3b).

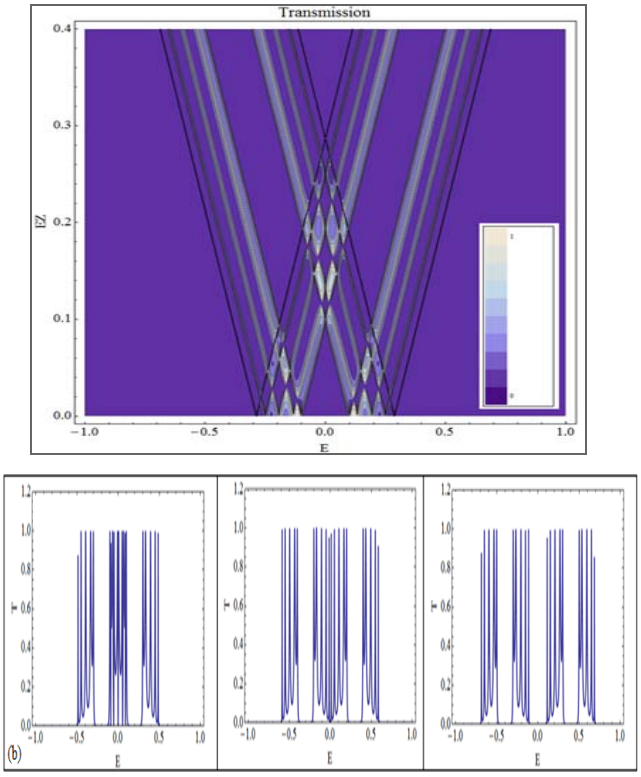

Figure 3. Plots for the five ring structure. (a) In the contour plot, transmission is plotted versus the Fermi energy (E) of the system and the value of Zeeman splitting energy (EZ) in the QD's in the arms of each ring. As the Zeeman splitting energy is increased, the system alternates between semiconductor and conductor. (b) Additional plots show the transmission for Zeeman splitting energies of 0.2, 0.3, and 0.4, from left to right.

Finally, we study the tunneling current of the multi-ring system by evaluating the current-voltage (*I-V*) characteristics with the transmission function $T(E)$, using the standard formalism based on the scattering theory of transport [8],

$$I = \frac{2e}{h}\int dE\,T(E)[f_L(E) - f_R(E)]\,. \qquad (2)$$

Here, $f(E)$ is the Fermi function given by $f_{L/R}(E) = \dfrac{1}{e^{\beta(E-\mu_{L/R})}+1}$, where $\beta = 1/k_BT$ and $\mu_{L/R}$ is the electrochemical potential of the left (right) semi-infinite leads, whose values depend on the applied source-drain bias voltage V_{sd}. We assume symmetric leads and set $\mu_L = eV_{sd}/2$, with the Fermi energy, $E_F = 0.0$.

In Fig. 4 (on last page), we see that with five rings, the I-V characteristics start to saturate, and thereafter do not change substantially with the addition of more rings in the chain. It is also evident that the splitting of the resonant peaks of the transmission due to the external magnetic field reduces the band gap of the system so that it effectively becomes a conductor for the value ZSE=ε_{QD}=0.1. Increasing ZSE further (ZSE > 0.3) eventually transitions the device back to semiconductor I-V characteristics.

IV. Conclusions

The multi-ring system with embedded QD's has semiconductor properties in the absence of any Zeeman splitting of the QD energy levels. The number of rings determines how well defined the band gap and conduction bands are, with more rings providing higher definition of these features. The inner edges of the gap sit roughly at the QD energy levels. The semiconductor properties of the transmission and its related I-V characteristics can be adjusted by changing the external magnetic field or parameters of the system. In particular, the system can be tuned from a semiconductor to conductor via the external magnetic field. The ability to switch from semiconductor to conductor may have useful applications in nano electronics.

References

[1] A. W. Holleitner, C. R. Decker, H. Qin, K. Eberl, and R. H. Blick, "Coherent coupling of two quantum dots embedded in an Aharonov-Bohm interferometer," Phys. Rev. Lett. **87**, 256802 (2001).

[2] E. R. Hedin, A. C. Perkins, and Y. S. Joe, "Combined Aharonov-Bohm and Zeeman spin-polarization effects in a double quantum dot ring," Physics Letters A, **375**, 651 (2011).

[3] E. R. Hedin, Y. S. Joe, and A. M. Satanin, "Sharpened Aharonov-Bohm oscillations near resonance in a balanced ring with double quantum dots," Jnl. Comput. Electron **7**, 280 (2008).

[4] E. R. Hedin and Y. S. Joe, "Sensitive spin-polarization effects in an Aharonov-Bohm double quantum dot ring," Jnl. of Appl. Phys. **110**, 026107 (2011).

[5] S. Das Sarma, "Spintronics," American Scientist, **89**, 516, (2001).

[6] R. Hanson, L. M. K. Vandersypen, L. H. Willems van Beveren, J. M. Elzerman, I. T. Vink, and L. P. Kouwenhoven, "Semiconductor few-electron quantum dot operated as a bipolar spin filter," Phys. Rev. B **70**, 241304(R) (2004).

[7] P. Recher, E. V. Sukhorukov, and D. Loss, "Quantum dot as spin filter and spin memory," Phys. Rev. Lett. **85**, 1962 (2000).

[8] S. Datta, Quantum Transport: Atom to Transistor (Cambridge University Press, New York, 2005).

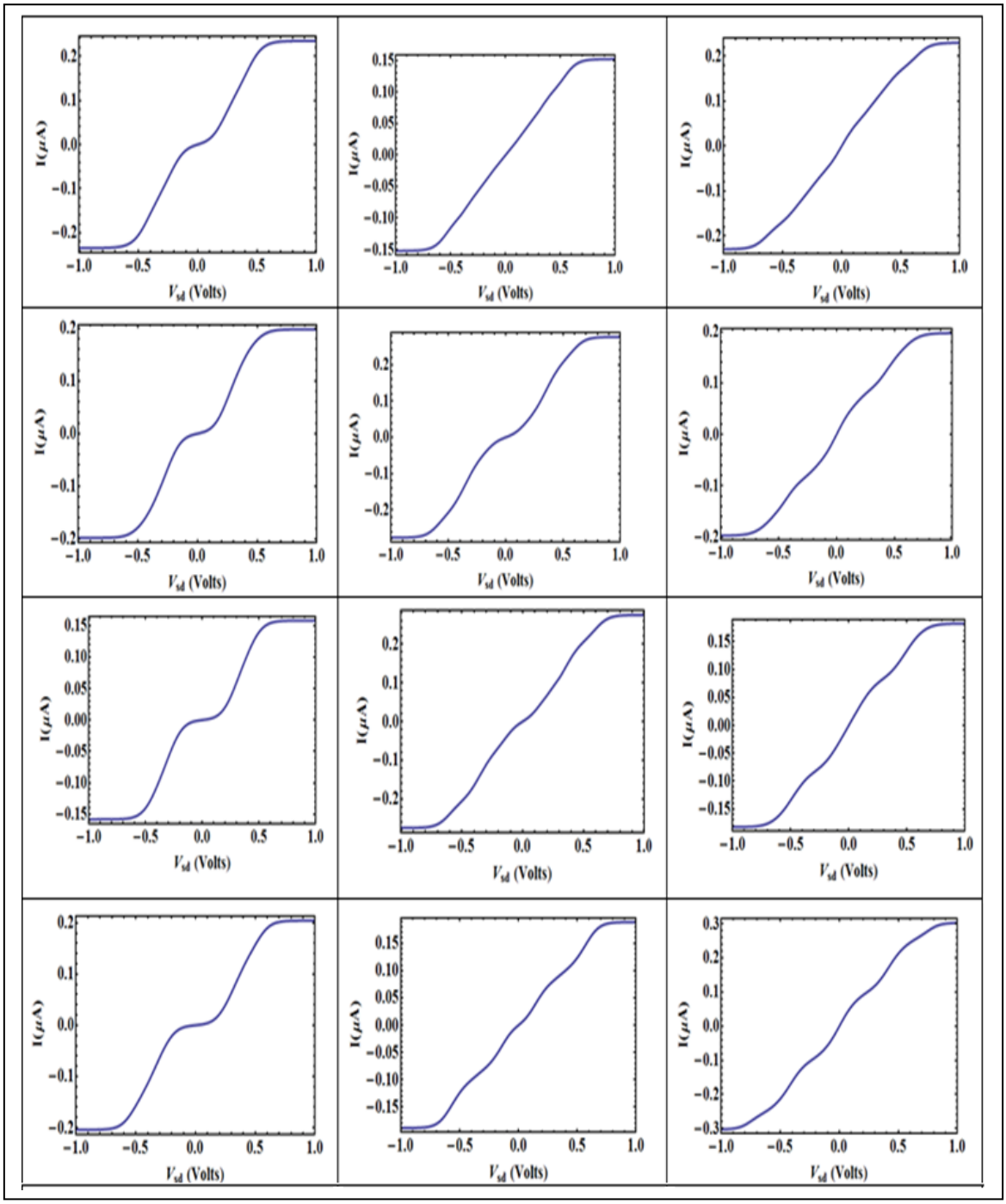

Figure 4. The conductance of the multi-ring system is plotted. The plots are arranged in parallel with Fig.2, and each conductance plot is associated with the same transmission plot. Adding more rings makes the system more distinctly a semiconductor, up to five. With more than five rings the system saturates and further change in the conductance is not as plainly seen.